



Satellite remote sensing of cloud base height for convective cloud fields:

A case study

Ralf Meerkötter¹ and Tobias Zinner^{1,2}

Received 23 April 2007; revised 21 June 2007; accepted 31 July 2007; published 5 September 2007.

[1] A method is proposed for estimating base heights of convective clouds from satellite data. The approach takes advantage of the fact that convective water clouds appear as geometrically and optically thin clouds near an approximately constant condensation level in their earliest stage of growth and that deriving geometrical thicknesses for such thin clouds is less error prone. Striking is the fact that the method also provides the base height for clouds with large vertical extensions and high optical thicknesses. The method has been applied to NOAA/AVHRR data of 20 selected cloud scenes. For an evaluation satellite retrieved cloud base heights have been compared to surface ceilometer measurements at the same time. First results are encouraging. The standard deviation of the differences between satellite and ceilometer measurements is $\pm 369\text{m}$ with no systematic bias. **Citation:** Meerkötter, R., and T. Zinner (2007), Satellite remote sensing of cloud base height for convective cloud fields: A case study, *Geophys. Res. Lett.*, *34*, L17805, doi:10.1029/2007GL030347.

1. Introduction

[2] Cloud properties play an essential role in the climate system since they influence the radiation budget at the top of the atmosphere as well as at the surface. The cloud base height (CBH) is of particular importance for the longwave radiation at the surface. CBH is not directly available from passive satellite observations and several approaches for retrieving CBH from active and passive satellite instruments have been proposed.

[3] Forsythe *et al.* [2000], for example, show that a satellite-based (GOES-8) cloud classification scheme combined with surface reports of the CBH yields an improvement over CBH estimates from surface reports alone. Minnis *et al.* [1995] introduced an operational retrieval of cloud base height based on the cloud top pressure and empirical assumptions on the cloud thickness in dependence on retrieved optical thickness, cloud top temperature, and cloud phase. This approach was recently improved by Chakrapani *et al.* [2002] but still has its largest uncertainties for optically thick clouds. Wilheit and Hutchison [2000] examined the use of a satellite-based combination of passive microwave (DMSP/SSM/T-2) brightness temperatures and infrared measurements (NOAA/AVHRR) of cloud top temperature for a CBH retrieval that is applicable over the

ocean. An approach for retrieving CBH of single layer water clouds and cirrus clouds using passive MODIS data is described by Hutchison [2002]. It is based on inferring the cloud geometrical thicknesses (CGT) from the cloud optical thickness (COT), the cloud effective radius (r_{eff}), and an assumption about the liquid water content (LWC). Hutchison [2002] shows that the accuracy in retrieving CBH depends on uncertainties in cloud top height (CTH), in the specification of LWC, and in the analysis of r_{eff} as well as of COT. For a 10% uncertainty in both, r_{eff} and COT, errors of about 20% result in the CGT estimation. Errors further grow (up to 100%) if an incorrect LWC is assumed.

[4] Bennartz [2007] used an approach similar to Hutchison [2002] and compared two years of microphysical parameters and CGT derived from global MODIS data for shallow marine stratocumulus over large areas in the Northern and Southern Hemisphere. He states that CGT can be derived with a relative uncertainty of better than 20% for cloud fractions higher than 0.8. Also focusing on small marine cumulus clouds Kassianov *et al.* [2003] present a retrieval for CGT based on multi-angle observations of the MISR instrument on the NASA Terra platform. This retrieval uses the dependence of cloud cover fraction changes with viewing angle due to vertical cloud structures. Evaluation of the method with a ground-based radar measurement and simulated MISR data for cloud fields from large eddy simulations indicate an accuracy of about 100 m in estimating the average CGT.

[5] We propose an approach for estimating the CBH of convective water clouds and apply it to data from the AVHRR sensor for which long-term data and cloud products exist [Meerkötter *et al.*, 2004]. The key idea of the method is to select only those clouds in a cloud field for retrieval that are in their earliest stage of growth, optically thin and located near the condensation level. Herewith, the method simultaneously provides the CBHs of existing geometrically and optically thick clouds. In the following we describe the approach, present results from its application to NOAA/AVHRR data and compare satellite-derived CBHs with surface ceilometer measurements.

2. Basic Assumptions

[6] Principle ideas underlying our approach are: convective clouds start growing at a rather fixed cumulus condensation level; convective clouds appear as geometrically and optically thin clouds in their earliest stage of growth; and the cumulus condensation level is nearly constant over large areas at any one time. These assumptions are valid for air masses widely unaffected by advective motions and forming homogeneous fields of vertical temperature and humid-

¹Institut für Physik der Atmosphäre, Deutsches Zentrum für Luft- und Raumfahrt, DLR, Oberpfaffenhofen, Germany.

²Temporarily at Nasa Goddard Space Flight Center, Greenbelt, Maryland, USA.

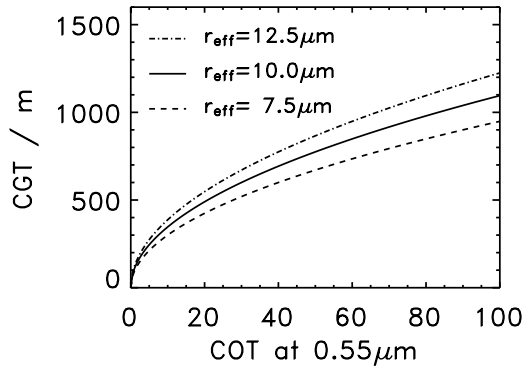


Figure 1. Relation between cloud geometrical thickness (CGT) and cloud optical thickness (COT) for adiabatic clouds with different effective radii r_{eff} .

ity profiles. For thin water clouds the assumption of an adiabatic vertical LWC is often satisfied and errors introduced by uncertainties in estimating the COT and microphysical parameters from satellite data remain small (shown below).

[7] The cloud base height (CBH) can be expressed as the difference of the cloud top height (CTH) and the cloud geometrical thickness (CGT):

$$CBH = CTH - CGT \quad (1)$$

[8] The relationship between CGT and COT for a range of effective radii (r_{eff}) is illustrated in Figure 1. The underlying adiabatic model is described in the next section. Note that thin clouds with COTs of 5 have CGTs at approximately 200 m. Figure 1 further demonstrates that uncertainties in the knowledge of r_{eff} lead to smaller uncertainties in CGT for optically thin clouds. For example, the variation of r_{eff} from 7.5 μm to 12.5 μm (5 to 15 μm) leads to a CGT difference of 74 m (152 m) at COT of 5. For COT of 40 the same variation in r_{eff} already leads to a CGT difference of 209 m (430 m).

3. Adiabatic Model

[9] An adiabatic model describes the vertical profile of cloud microphysics assuming that a saturated cloud air parcel is lifted adiabatically from the cloud base height without exchange of heat with the surrounding air. It is an approximation of real conditions but it is justified in the early stages of convective cloud growth before either collisional growth of droplets or strong mixing due to strong turbulence occur.

[10] In an adiabatic cloud layer *Brenguier et al.* [2000] show that COT is related to droplet number density N ($1/\text{cm}^3$) and CGT via:

$$COT = 3/5\pi Q_{\text{ext}} [C_w / (4/3\pi\rho)]^{2/3} (kN)^{1/3} CGT^{5/3} \quad (2)$$

[11] The factor k represents the ratio of the mean volume radius (r_{vol}) of a droplet spectrum and the effective radius, $r_{\text{vol}}^3/r_{\text{eff}}^3$ [e.g., *Martin et al.*, 1993], C_w is a condensation coefficient that linearly relates the adiabatic LWC to the CGT, ρ denotes the density of water (1 g/cm^3), Q_{ext} is the

extinction efficiency. The relation between N , r_{eff} , and CGT can be expressed as:

$$N = C_w CGT / \left(4/3\pi\rho k r_{\text{eff}}^3 \right) \quad (3)$$

[12] Inserting (3) into (2) to eliminate N and approximating Q_{ext} by 2, which is valid for droplets much larger than the wavelength, an expression is obtained for CGT as a function of COT, r_{eff} , and C_w :

$$CGT = [10/9 COT \rho r_{\text{eff}} / C_w]^{1/2} \quad (4)$$

[13] The constant C_w is expressed as a function of temperature and pressure near the cloud base [e.g., *Brenguier et al.*, 2000; *Zinner et al.*, 2006]. In this study COT and cloud top temperature (T_{top}) have been derived from NOAA/AVHRR data by use of the APOLLO processing scheme [*Kriebel et al.*, 1989, 2003; *Meerkötter et al.*, 2004]. COT is based on reflectivities derived from radiance measurements in AVHRR channel 1 and T_{top} is derived from measured radiances in the thermal AVHRR channels. Note that APOLLO calculates COT for totally cloud covered pixels only. The spatial resolution of the AVHRR instrument is $\sim 1 \text{ km}$ at the sub-satellite point. Pixels identified as ice clouds or being partially cloudy at this $\sim 1 \text{ km}$ resolution have been excluded from this study.

[14] Since the approach of estimating CBH is based on optically and thus geometrically thin water clouds, temperature and pressure retrieved for the cloud top are used for C_w . The pressure is obtained from T_{top} and heights provided by radiosonde profiles. We assume a fixed value of $r_{\text{eff}} = 10 \mu\text{m}$ since uncertainties in r_{eff} and their effect on CBH estimations remain relatively small for optically thin clouds (Figure 1).

4. Application to Measured Data

[15] Our procedure for retrieving cloud base heights from satellite and auxiliary data can be summarized by the following steps: (1) In selected scenes of broken clouds all totally cloudy AVHRR pixels with $5 \leq COT \leq 7$ are extracted by using the APOLLO processing scheme. (2) For these pixels T_{top} is estimated from AVHRR thermal radiances. (3) Each T_{top} is assigned to a CTH by the aid of a radiosonde profile. (4) CGT values are inferred according to (4), i.e., based on the adiabatic model, with COT values from step 1, and by using a prescribed value of $r_{\text{eff}} = 10 \mu\text{m}$. (5) For each totally cloudy pixel the CBH is estimated according to (1). (6) CBH values are spatially averaged over a selected area.

[16] Note that $5 \leq COTs \leq 7$ are necessary for reasonable cloud top temperature retrievals. CBH values have been estimated with this algorithm for 20 NOAA/AVHRR scenes over southern Germany containing convective broken clouds. The main criterion for the selection of these scenes was the existence of a single layer cloud field. These scenes were identified by analyzing NOAA images and histograms of T_{top} , as well as by analyzing available ceilometer data.

[17] The NOAA/AVHRR data are from different months in the years 2002 and 2003 with a range of different CBH values. Southern Germany was chosen for the validation

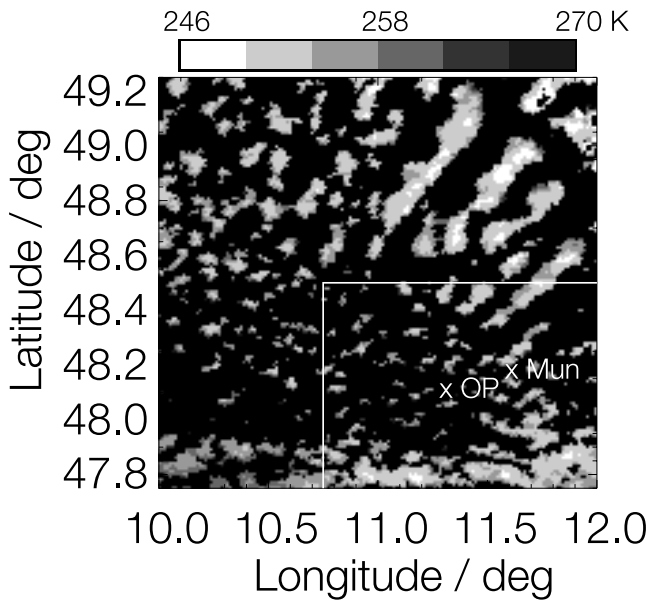


Figure 2. Example of a broken cloud scene over southern Germany on April 6, 2003, at 12:06 UTC. Shown is the distribution of T_{top} . CBHs are retrieved and averaged over the framed area. OP denotes the location of the DLR ceilometer near Oberpfaffenhofen and Mun denotes the location of the radiosonde station near Munich, about 30 km from the OP site.

and because ceilometer measurements are obtained at the Deutsches Zentrum für Luft- und Raumfahrt (DLR) near Oberpfaffenhofen. Since 1998 a modified Vaisala ceilometer has been operating 24 hours a day at DLR, producing vertical backscatter profiles every 30 s. The system contains a laser operating at a 900 nm wavelength with a peak pulse power of 30 W. Radiosonde profile measurements were performed at the station Oberschleißheim near Munich at a distance of about 30 km from the ceilometer site. Radiosondes with launch times at 12:00 UTC were used in this study together with AVHRR overpasses between 11:46 UTC and 13:03 UTC. Figure 2 presents an example of a broken cloud field and marks the locations of the radiosonde and ceilometer sites.

5. Results

[18] Analyzing the histograms of T_{top} for all selected cloud scenes confirms that observed geometrically thin convective clouds are in fact those that start growing from a cloud base height common to the whole cloud field. Comparing two histograms of T_{top} for each scene (not shown), one representing all totally cloudy pixels with $COT \geq 5$ and the other representing thin water clouds, i.e. all totally cloudy pixels with $5 \leq COT \leq 7$, reveals that average T_{top} values are always shifted towards higher temperatures for $5 \leq COT \leq 7$. This indicates that the CTHs of the thinner clouds are located at lower, and thus warmer, atmospheric levels. The shift depends on the average CGT of the cloud field ranging between about 2 K and 7 K for the selected scenes.

[19] As an example, Figure 3 shows a satellite derived CBH value in conjunction with the time series of the

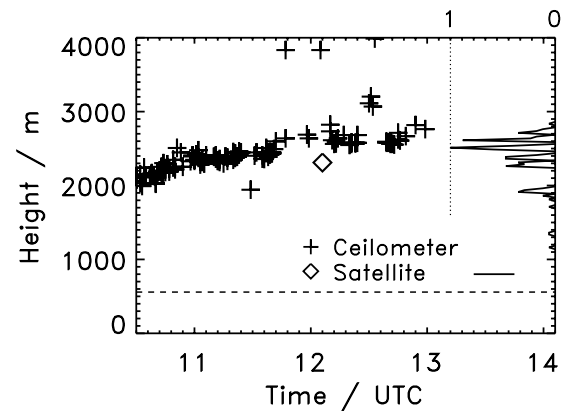


Figure 3. Example of a satellite estimate of CBH (above MSL) in comparison to ceilometer heights as a function of daytime on April 6, 2003 (symbols). The normalized histogram at the right axis shows a temporal (overpass time ± 0.5 h) distribution of the satellite retrieved base height. The horizontal dashed line denotes the ceilometer altitude of 558 m above MSL.

ceilometer, here for April 6, 2003. The ceilometer heights show a clearly marked CBH and a typical increase in CBH during the day with small variations. Some ceilometer heights occur at higher levels. The radiosonde data show a weak inversion layer at about 3800 m which points to residuals of clouds evaporating below the inversion at the end of their individual lifecycle.

[20] Convective cloud fields naturally appear in a broad range of different 3-dimensional structures. We compare CBH values derived from NOAA/AVHRR data with ceilometer measurements for cloud scenes selected from 20 different days (Figure 4). Also displayed are mean and maximum CTH values derived from the satellite observed T_{top} . The CBHs from the ceilometer measurements represent temporal averages over a time interval of ± 30 minutes centered on the local NOAA overpass time, whereas the satellite-derived geometrical cloud parameters are spatial averages over the sub-area indicated in Figure 2.

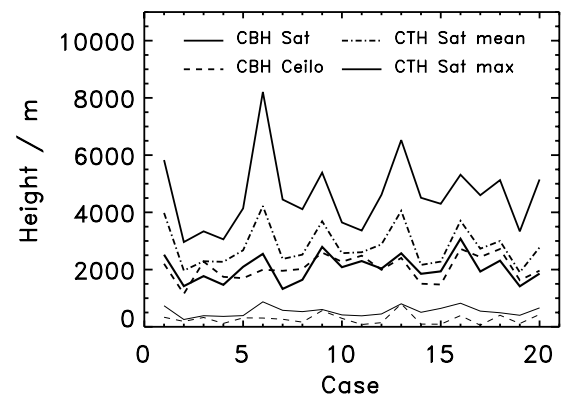


Figure 4. CBHs from satellite and ceilometer measurements, as well as the mean and maximum CTHs from the satellite method, for 20 cloud scenes. The lower two curves represent standard deviations of the ceilometer and the satellite-based estimates in corresponding line styles.

[21] The standard deviation of the 20 differences $\Delta\text{CBH} = \text{CBH}_{\text{sat}} - \text{CBH}_{\text{ceilo}}$ is ± 369 m, with the average of the 20 differences at -15 m. The bias at -15 m is much less than the standard deviation in the differences and not significant. The relation between ceilometer and satellite-based results is expressed in a correlation coefficient of 0.68. The current study is based on spatially and temporally averaged CBH values. It would be interesting to analyze individual clouds, that is to compare CBH estimates for single clouds with simultaneous ceilometer measurements. The CTH values in Figure 4, and especially the maxima, indicate that it is possible to derive the CBHs of a convective cloud field by analyzing optically thin water clouds of the field only, even if the cloud field contains geometrically and optically very thick clouds.

[22] For an explanation of the differences between satellite and ceilometer measurements several sources of error should be taken into account.

[23] Kriebel *et al.* [1989] have estimated that the COT estimated with the APOLLO scheme has an error of about $\pm 30\%$. Provided that a fixed r_{eff} is uncertain by about $\pm 25\%$, the errors that result in CGT using (4) is about $\pm 28\%$. However, assuming for example, a CBH at ~ 2000 m and a CGT on the order of 200 m (COT $\sim 5-7$), these uncertainties in COT and r_{eff} amount to errors of $\sim 3\%$ for the CBH estimation.

[24] The accuracy of the DLR ceilometer corresponds to its vertical resolution which in turn is determined by the specific pulse width (20 ns) and the sampling rate (20 MHz). For hard targets this results in a vertical resolution of 7.5 m. For the detection of softer targets as boundary layer water clouds signal to noise thresholds and a defined number of consecutive samples (here 3) above a threshold are applied. This leads to a vertical resolution of 22.5 m at best.

[25] The differences $\Delta\text{CBH} = \text{CBH}_{\text{sat}} - \text{CBH}_{\text{ceilo}}$ obtained for the selected 20 cases are most likely explained by the natural variability of the CBH, by uncertainties in deriving the cloud top temperature T_{top} , and by uncertainties in relating T_{top} to a cloud top height. Uncertainties in the radiosonde measurements and sampling issues between the ceilometer and AVHRR display a role. Errors in satellite derived T_{top} values are predominantly caused by geometrical cloud top structures inside a pixel, which may lead to lesser uncertainties for shallow clouds than for vertically extended clouds (e.g., cumulus congestus). Horizontal inhomogeneities in temperature and humidity and their influence on the spatial distributions of CBHs may, in some cases, not be adequately represented by temporally averaged ceilometer point measurements.

6. Conclusions

[26] An approach for estimating cloud base heights in broken convective cloud fields using satellite data has been proposed. Its utility has been demonstrated by its application to AVHRR data and comparison of its results with surface ceilometer measurements. The approach is confined to convective clouds and may serve as a complement to other methods treating different cloud types.

[27] The method can, in principle, be applied to all satellite instruments that are capable of providing cloud optical thickness and cloud top temperature. Although not necessarily needed, a satellite-derived effective radius would further reduce the uncertainties associated with the retrieval. The method is applicable to data from the SEVIRI instrument onboard the European geostationary satellite Meteosat/8, to AVHRR/3 data from the MetOp-A satellite and to MODIS data from the NASA Terra and Aqua satellite.

[28] Next steps in further developing and testing the method will focus on extending the number of test scenes with respect to season and region. After this, an application to a long-term satellite data set is targeted.

[29] **Acknowledgments.** We are grateful to J. Streicher (DLR) for making available the ceilometer data. K. Gierens and B. Mayer (both DLR) we thank for their constructive and helpful comments.

References

- Bennartz, R. (2007), Global assessment of marine boundary layer cloud droplet number concentration from satellite, *J. Geophys. Res.*, *112*, D02201, doi:10.1029/2006JD007547.
- Brenguier, J.-L., H. Pawlowska, L. Schüller, R. Preusker, J. Fischer, and Y. Fouquart (2000), Radiative properties of boundary layer clouds: Droplet effective radius versus number concentration, *J. Atmos. Sci.*, *57*, 803–821.
- Chakrapani, V., D. R. Doelling, A. D. Rapp, and P. Minnis (2002), Cloud thickness estimation from GOES-8 satellite data over the ARM-SGP site, paper presented at the Twelfth ARM Science Meeting, Atmos. Radiat. Meas. Program Sci. Team, St. Petersburg, Fla., 8–12 Apr.
- Forsythe, J. M., T. H. Vonder Haar, and D. L. Reinke (2000), Cloud-base height estimates using a combination of meteorological satellite imagery and surface reports, *J. Appl. Meteorol.*, *39*, 2336–2347.
- Hutchison, K. D. (2002), The retrieval of cloud base heights from MODIS and three-dimensional cloud fields from NASA's EOS Aqua mission, *Int. J. Remote Sens.*, *23*(24), 5249–5265.
- Kassianov, E., T. Ackerman, R. Marchand, and M. Ovtchinnikov (2003), Satellite multangle cumulus geometry retrieval: Case study, *J. Geophys. Res.*, *108*(D3), 4117, doi:10.1029/2002JD002350.
- Kriebel, K. T., R. W. Saunders, and G. Gesell (1989), Optical properties of clouds derived from fully cloudy AVHRR pixels, *Contrib. Atmos. Phys.*, *62*(3), 165–171.
- Kriebel, K. T., G. Gesell, M. Kästner, and H. Mannstein (2003), The cloud analysis tool APOLLO: Improvements and validations, *Int. J. Remote Sens.*, *24*(12), 2389–2408.
- Martin, G. M., D. W. Johnson, and A. Spice (1993), The measurement and parameterization of effective radius of droplets in warm stratocumulus clouds, *J. Atmos. Sci.*, *51*, 1823–1842.
- Meerkötter, R., C. König, P. Bissolli, G. Gesell, and H. Mannstein (2004), A 14-year European Cloud Climatology from NOAA/AVHRR data in comparison to surface observations, *Geophys. Res. Lett.*, *31*, L15103, doi:10.1029/2004GL020098.
- Minnis, P., D. P. Kratz, J. A. Coakley Jr., M. D. King, D. Garber, P. Heck, S. Mayor, D. F. Young, and R. Arduini (1995), Cloud Optical Property Retrieval (Subsystem 4.3), in *Clouds and the Earth's Radiant Energy System (CERES) Algorithm Theoretical Basis Document, Volume III: Cloud Analyses and Radiance Inversions (Subsystem 4)*, edited by CERES Science Team, NASA RP 1376, pp. 135–176, NASA Res. Cent., Hampton, Va.
- Wilheit, T. T., Jr., and D. Hutchison (2000), Retrieval of cloud base heights from passive microwave and cloud top temperature data, *IEEE Trans. Geosci. Remote Sens.*, *38*(3), 1253–1259.
- Zinner, T., B. Mayer, and M. Schröder (2006), Determination of three-dimensional cloud structures from high-resolution radiance data, *J. Geophys. Res.*, *111*, D08204, doi:10.1029/2005JD006062.

R. Meerkötter and T. Zinner, Institut für Physik der Atmosphäre, Deutsches Zentrum für Luft- und Raumfahrt, DLR, Oberpfaffenhofen, D-82234 Wessling, Germany. (ralf.meerkotter@dlr.de; tobias.zinner@dlr.de)